JOURNAL OF VIROLOGY, Aug. 1990, p. 3661–3673
0022-538X/90/083661-13$02.00/0

Vol. 64, No. 8

# Human Adenovirus-Host Cell Interactions: Comparative Study with Members of Subgroups B and C

CHRISTINE DEFER,[1] MARIE-THÉRÈSE BELIN,[1] MARIE-LAURE CAILLET-BOUDIN,[1] AND PIERRE BOULANGER[2]*

*Unité de Virologie Moléculaire de l'Institut National de la Santé et de la Recherche Médicale, (U-233), 59045 Lille,[1] and Laboratoire de Virologie et Pathogénèse Moléculaires, Faculté de Médecine, Boulevard Henri IV, 34060 Montpellier,[2] France*

Received 9 February 1990/Accepted 8 May 1990

**Host cell interactions of human adenovirus serotypes belonging to subgroups B (adenovirus type 3 [Ad3] and Ad7) and C (Ad2 and Ad5) were comparatively analyzed at three levels: (i) binding of virus particles with host cell receptors; (ii) cointernalization of macromolecules with adenovirions; and (iii) adenovirus-induced cytoskeletal alterations. The association constants with human cell receptors were found to be similar for Ad2 and Ad3 ($8 \times 10^9$ to $9 \times 10^9$ $M^{-1}$), and the number of receptor sites per cell ranged from 5,000 (Ad2) to 7,000 (Ad3). Affinity blottings, competition experiments, and immunofluorescence stainings suggested that the receptor sites for adenovirus were distinct for members of subgroups B and C. Adenovirions increased the permeability of cells to macromolecules. We showed that this global effect could be divided into two distinct events: (i) cointernalization of macromolecules and virions into endocytotic vesicles, a phenomenon that occurred in a serotype-independent way, and (ii) release of macromolecules into the cytoplasm upon adenovirus-induced lysis of endosomal membranes. The latter process was found to be type specific and to require unaltered and infectious virus particles of serotype 2 or 5. Perinuclear condensation of the vimentin filament network was observed at early stages of infection with Ad2 or Ad5 but not with Ad3, Ad7, and noninfectious particles of Ad2 or Ad5, obtained by heat inactivation of wild-type virions or with the H2 *ts*1 mutant. This phenomenon appeared to be a cytological marker for cytoplasmic transit of infectious virions within adenovirus-infected cells. It could be experimentally dissociated from vimentin proteolysis, which was found to be serotype dependent, occurring only with members of subgroup C, regardless of the infectivity of the input virus.**

Human adenoviruses are nonenveloped, DNA-containing icosahedral viruses. Besides the obvious interest in viruses with respect to clinical and molecular pathology, human adenoviruses in particular have often been considered invaluable for studies of cellular processes. Human adenovirus serotypes 2 and 5 (Ad2 and Ad5) and their mutants have been widely used as molecular probes for studying class II and class III gene expression in eucaryotic cells (reviewed in references 5 and 20). Furthermore, the adenovirus genome contains oncogenes, a peculiarity that has led several groups to use adenovirus-transformed cells as a model system for malignant transformation in vitro (58, 67).

Recent studies have shown that virus infection permeabilizes mammalian cells to antibiotics or proteinic toxins that are unable to enter normal cells (11, 12, 18, 19, 45). This phenomenon has also been documented with human adenovirus (19, 45, 54–56, 70). Adenovirus has been found to increase cell membrane permeability to macromolecules and sensitivity of cells to toxins. Adenovirus particles and toxins, e.g., *Pseudomonas* exotoxin (19, 54) and α-sarcin (45), or fluorescent dextran (70), are cointernalized at early stages of infection, following the common pathway of entry of macromolecules into animal cells (25, 26).

The internalization pathway of adenovirus can be summarized as follows: (i) recognition and attachment of the virions to the receptors present at the cell surface (8, 9, 32, 40, 48, 61, 62); (ii) clustering of receptors at the cell surface (28, 29, 47, 57) and their invagination into a coated pit; (iii) internalization of the virus particles bound to the membrane receptors via a clathrin-coated vesicle (55); (iv) dissociation of the clathrin coat to generate an endocytotic vesicle (25, 26); (v) decrease of intravesicular pH by a proton pump present in the endosomal membrane (59, 69); (vi) occurrence of conformational changes in the capsid as a result of acidification of the endosome content, provoking the release of altered virions into the cytoplasm (41, 54, 56); and (vii) transfer of the virions to the nucleus.

Most of the internalization studies thus far reported have concerned Ad2 and Ad5, both belonging to subgroup C (68). However, the serotypes mainly involved in human pathology are other serotypes, belonging to subgroups B and F. Serotype 3 (subgroup B) is most frequently associated with acute respiratory diseases in children (37, 53). The fastidious serotypes 40 and 41 (subgroup F) are found in acute infantile gastroenteritis (2, 31, 63, 64). These findings prompted us to reinvestigate the penetration routes of serotypes other than the two well-known serotypes 2 and 5. We therefore analyzed the early interactions between host cells and serotypes 3 and 7 in comparison with serotypes 2 and 5.

We find that the membrane receptor components recognized by the infectious adenovirus particles, the transcytoplasmic routes, and the alterations of the cytoskeletal network associated with adenovirus infection are different for members of subgroups B and C. Using different adenovirus serotypes and some of their mutants, we also provide experimental evidence that the perinuclear condensation of the vimentin filament network that we observe in cells early after infection can be experimentally dissociated from the

* Corresponding author.

adenovirus-induced proteolysis of vimentin that we have recently described (4). In addition, we show that the increased endocytosis of impermeable macromolecules cointernalized with adenovirus and the extent of release of virus particles from endocytotic vesicles into the cytoplasm are uncoupled phenomena. The results presented here therefore have implications for both cell physiology and viral pathogenesis.

## MATERIALS AND METHODS

**Cells.** Human cell lines KB, HeLa, HEp-2, A549, and HEK-293 were cultured as monolayers in Eagle minimal essential medium supplemented with 5% fetal calf serum and 5% γ-irradiated newborn calf serum. A549 is an established cell line derived from human lung carcinoma (22; CCL 185). Production of adenovirus in high yields was performed in KB cells grown in suspension at a density of $2 \times 10^5$ to $5 \times 10^5$ cells per ml in Joklik-modified medium (F13; Difco Laboratories, Detroit, Mich.) supplemented with 5% horse serum.

**Virus and virus infection.** Wild-type (WT) human Ad2 and Ad5 (subgroup C) and Ad3 and Ad7 (subgroup B) were produced in suspension-grown KB cells. Mutant H5 *dl*312, deleted in the E1A region (30), was produced in HEK-293 cells. Temperature-sensitive mutant H2 *ts*1 was originally obtained from J. Weber. It has been shown to be altered in the virus-coded protease (1, 6, 33, 38). H2 *ts*1 stocks were produced at 32°C (permissive temperature); noninfectious H2 *ts*1 particles (containing uncleaved protein precursors [15]) were produced at 39°C. The virus titers were determined by a fluorescent focus assay as previously described (17) and expressed as fluorescent focus units (FFU). Unless otherwise indicated, cells were infected at a multiplicity of infection (MOI) of 10 to 25 FFU per cell. In all studies of binding with the cell receptors and of endocytosis of virions, the input of physical particles (total infectious plus noninfectious virions) was determined by protein assay (66) and indicated in each experiment. Adenovirions were isolated as previously described (17).

**Radioactive and fluorescent labeling of adenovirus particles.** Virions were radioactively labeled in their DNA by addition of [$^3$H]thymidine (27 Ci/mmol; CEA, Saclay, France) at 1 mCi/ml for 20 h at 10 h after infection in serum-deprived infected-cell cultures. The specific radioactivity was usually $2 \times 10^6$ to $5 \times 10^7$ cpm per $10^{13}$ virions. Labeling of viral proteins was carried out with [$^{14}$C]valine (2.5 μCi/ml) for 13 h at 17 h after infection. [$^{14}$C]valine (275 mCi/mmol; CEA) was added to infected-cell cultures maintained in a serum-free medium containing 10% the concentration of valine in normal medium. Rhodamine labeling of adenovirions was performed by the method described by Persson et al. (47), with minor modifications. Tetraethylrhodaminylisothiocyanate (TRITC) was purchased from Sigma Chemical Co. (St. Louis, Mo.).

**Binding experiments.** Adenovirus was attached to KB or A549 cells according to a procedure derived from the one developed by Persson et al. (47, 48). Cells were washed once in phosphate-buffered saline (PBS) and suspended to $3 \times 10^6$ cells per ml. Samples (100 μl) of the cell suspension ($3 \times 10^5$ cells) were mixed with 100 μl of [$^3$H]thymidine-labeled virions, and the virus-cell mixture was incubated for 45 min at 20°C. At this temperature, mainly adsorption and very little penetration have been shown to occur (47, 48). Ratios of physical particles to cell number varied from 5,000 to 300,000 in the inoculum, with a specific radioactivity of $5 \times 10^7$ cpm per $10^{13}$ virions. The cells were then sedimented and rinsed once with PBS. The two supernatants were pooled and precipitated with 10% trichloroacetic acid for 30 min at 0°C. The precipitate was collected on a GF/C glass fiber filter and counted in a liquid scintillation spectrometer. This material is referred to as unadsorbed virus particles. The cell pellet was allowed to dissolve in 5% Sarkosyl–2% pronase for 24 h at 37°C; the acid-precipitable radioactivity is referred to as cell-adsorbed virions. Correction for quenching was performed by counting known amounts of acid-precipitable radioactivity of $^3$H-labeled virions mixed to prefractionated cell samples under the same conditions. Adenovirus binding data were graphically represented (51). The affinity of the receptor sites for adenovirions was derived from the slope of the Scatchard plot, its intercept with the abscissa giving the number of receptor sites per cell. As an example of calculation of apparent association constant ($K_{app}$) on a per-receptor-site basis (47), $5 \times 10^3$ adenovirus receptor sites per cell in a 0.2-ml sample containing $3 \times 10^5$ cells would correspond to $7.5 \times 10^{12}$ sites per liter, viz., a molarity of $1.25 \times 10^{-11}$ M in terms of receptor sites (see Fig. 1).

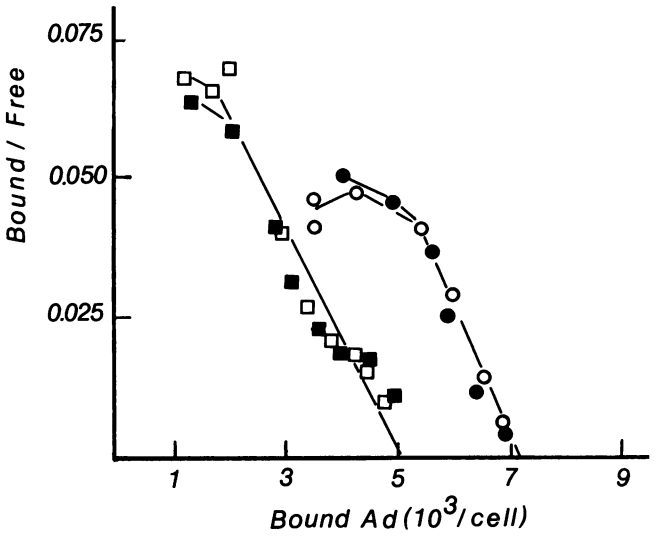


FIG. 1. Scatchard plot analysis of data for binding of adenovirus with KB and A549 cells. Increasing amounts of [$^3$H]thymidine-labeled virions of Ad2 (□ and ■) or Ad3 (○ and ●) were incubated with samples of cell cultures ($3 \times 10^5$ cells) for 45 min at 20°C. Ratios of bound to free virus label were plotted versus numbers of bound virus particles per cell. Open symbols, KB cells; filled symbols, A549 cells. The binding constants were derived from the slopes of the curves, and the number of receptor sites per cell was derived from the *x* intercept.

**Cell fractionation and virus compartmentalization.** Cells were incubated with $^3$H-labeled virus for 45 min at 37°C to allow penetration to occur. The quantity of virions in different cell compartments was assayed by counting the radioactivity in the following cellular fractions (3, 36). (i) Cytosolic fraction was recovered in the supernatant of cell lysis with alkaline hypotonic buffer (ATE buffer; 10 mM Tris hydrochloride [pH 8.9], 1 mM EGTA, 0.1 mM phenylmethylsulfonyl fluoride, 0.1 mM tosyl-L-phenylalanyl chloromethyl ketone). (ii) Endosomal vesicles and endoplasmic membranes were extracted from the pellet with TKMT buffer (50

mM Tris hydrochloride [pH 7.4], 25 mM KCl, 5 mM $MgCl_2$, 0.5% Triton X-100). (iii) Cytoskeletal elements unsoluble under these conditions and present within the resulting pellet were solubilized in TKMT buffer containing 0.5% Sarkosyl. (iv) The residual pellet contained nuclei, insoluble cell organelles, and matrix.

**Immunofluorescence microscopy. (i) Capping of adenovirus particles at the cell surface.** Infection with TRITC-conjugated adenovirus particles was conducted as follows. Cells were incubated with adenovirus inoculum for 30 min at 4°C and at 2,500 to 5,000 physical particles per cell. The cultures were then transferred to 37°C and harvested at the indicated times, from 5 to 45 min. The cells were extensively rinsed in PBS, fixed with 0.15% glutaraldehyde–4% paraformaldehyde in PBS, and examined by fluorescence microscopy.

**(ii) Analysis of internalized fluorescence-conjugated macromolecules.** A549 cell monolayers were infected with an adenovirus suspension (2,500 to 5,000 physical particles per cell) in PBS containing fluorescein isothiocyanate-labeled dextran (FITC-dextran; 10 mg/ml) or rhodamine isothiocyanate-labeled horseradish peroxidase (RITC-HRP; 2 mg/ml). After incubation at 37°C for 30 min, the cells were washed five times with PBS, fixed with 0.15% glutaraldehyde–4% paraformaldehyde in PBS for 30 min, rinsed in PBS, and examined by fluorescence microscopy. FITC-dextran and RITC-HRP were both purchased from Sigma.

**(iii) Observation of vimentin filament network.** Cells were fixed and permeabilized by the technique described by Langanger et al. (35) and then incubated with a mouse monoclonal anti-human vimentin serum (Monosan F3005; Sanbio Biological Products, Uden, Netherlands). The antigen-antibody complexes were revealed by an anti-mouse immunoglobulin G serum (FITC-labeled sheep anti-mouse heavy-plus-light-chain immunoglobulin G; Biosys, Compiègne, France).

**(iv) Lights, filters, and photomicrographs.** Stained cells and internalized fluorescent macromolecules were examined in an Olympus BH-2 microscope with the following wavelengths and filters: for rhodamine-labeled molecules, 530 to 560 nm for the excitation wavelength and edge filter at 580 nm; for fluorescein-labeled molecules, excitation at 270 to 280 nm and edge filter at 410 to 480 nm. Photomicrographs were taken with Kodak Ektachrome film (400 ASA).

**HRP assay.** The HRP assay was designed to quantitatively determine the amount of RITC-HRP cointernalized with adenovirus particles. RITC-HRP was used to provide a visual control of entry of HRP into cells by immunofluorescence microscopy of duplicate cell samples. A549 cell monolayers or KB cells in suspension were incubated without or with different adenovirus serotypes (5,000 physical particles per cell) for 30 min at 37°C in the presence of RITC-HRP (2 mg/ml). The cells were then rinsed with PBS maintained at 4°C and lysed in a 0.05% (vol/vol) solution of Triton X-100 in water. Peroxidase activity was assayed in cell lysates by the method of Otero and Carrasco (45). The substrate used was *o*-dianisidine, whose oxidized form gives a maximum absorbance at 460 nm. The results were expressed as enzymatic units per nanogram of cell protein. Standard curves of $A_{460}$ versus concentrations of freshly prepared HRP solutions were plotted in each experiment.

**Protein assays.** Protein concentration was determined by the spectrophotometric method of Whitaker and Granum (66).

**Isolation of KB cell plasma membranes.** Plasma membranes were isolated by two successive cycles of discontinuous sucrose gradients as previously described (27). In a typical experiment, 2 liters of KB cell spinner culture at a density of $5 \times 10^5$ cells per ml was centrifuged, washed in PBS, and lysed in 7 ml of 10 mM Tris hydrochloride buffer (pH 7.4) containing 10 mM NaCl and 1.5 mM $MgCl_2$ for 10 min at 0°C. The cell lysate was homogenized in a tight-fitting Dounce homogenizer; then 1 ml of a 80% (wt/vol) sucrose solution in 10 mM Tris hydrochloride (pH 7.4)–5 mM $MgCl_2$ was added to the homogenate, and the resulting suspension was loaded on top of a discontinuous gradient of sucrose (50%/30%) in the same buffer and centrifuged for 15 min at 4°C and 1,500 $\times$ *g*. Plasma membranes band at the 30%/50% interface.

**Polyacrylamide gel electrophoresis and ligand affinity blotting.** Unlabeled plasma membrane proteins were analyzed in 15.5% sodium dodecyl sulfate (SDS)-polyacrylamide gel electrophoresed in the discontinuous buffer system of Laemmli (34) and electrically transferred to nitrocellulose membrane filters (Transblot 0.45; Bio-Rad Laboratories, Richmond, Calif.) in 25 mM Tris–150 mM glycine–10% methanol at 200 mA for 3 h at room temperature. Blotted receptor components were probed with [$^{14}$C]valine-labeled adenovirus suspension ($10 \times 10^6$ cpm per 15- by 15-cm blot) in a ligand overlay buffer (3, 21, 46). KB cell membrane polypeptides possessing an affinity for adenovirions were detected by autoradiography. Since some major sticky host cell proteins might bind nonspecifically to adenovirions, we developed the technique of ligand overlay competition blotting. Blots of plasma membrane polypeptides were first saturated with mouse anti-cytoskeletal protein antibody (e.g., antiactin or antivimentin immunoglobulin) or reacted with unlabeled fiber. In the second step, the same blots were incubated with [$^{14}$C]valine-labeled adenovirus. Immunoblotting analysis of vimentin and actin proteins from cell extracts has been described in detail elsewhere (4). Mouse monoclonal anti-human vimentin (Monosan F 3005) and anti-rat actin (Monosan SK 4001) antibodies were both purchased from Sanbio Biological Products.

## RESULTS

**Cellular adsorption and penetration of different adenoviruses of subgroups B and C. (i) Determination of the infectivity efficiency for human Ad2, Ad3, Ad5, and Ad7 in human cells.** Since our study concerned adsorption, penetration, and intracellular migration of adenovirus particles of various serotypes, it was of major importance to determine their respective infectivity efficiencies, i.e., the ratio of infectious to physical virus particles (52). Table 1 shows comparative data obtained with KB and A549 cells. For the same virus inoculum, infectious titers varied from one cell type to another and were always significantly higher (5- to 20-fold) with A549 cells. For the same cell line, infectivity efficiency also varied with the serotype of infecting adenovirus, ranging from 1:10 to 1:20 for the members of subgroup C on A549 cells and from 1:50 to 1:100 on KB cells. For serotypes 3 and 7 (subgroup B), the infectivity efficiency was found to be considerably lower, ranging from 1:1,700 to 1:8,000 on KB cells and from 1:200 to 1:400 on A549 cells. Again, the infectious titers were consistently higher on A549 cells, regardless of the adenovirus serotype. HeLa cell monolayers gave the same results as KB cell monolayers (data not shown). Our results were reminiscent of previous data showing that the virion-to-PFU ratios ranged from 11:1 for Ad1 (subgroup C) to 2,300:1 for Ad25 (subgroup D) on KB cell monolayers (23). Similarly, a value of 200:1 for Ad7 on HEp-2 cells has been reported (16).

TABLE 1. Infectivity efficiency of various adenovirus serotypes on KB and A549 cells[a]

| Serotype | Inoculum ($10^{13}$ PP/ml)[b] | Infectious titer of inoculum[c] | | | |
|---|---|---|---|---|---|
| | | KB | | A549 | |
| | | FFU/ml (mean ±SEM) | R | FFU/ml (mean ± SEM) | R |
| Ad2 | 4.5 | $5.1 \pm 1.3 \times 10^{11}$ | 95 ± 33 | $5.5 \pm 2.2 \times 10^{12}$ | 9 ± 3 |
| Ad2 | 4.4 | $4.2 \pm 1.3 \times 10^{11}$ | 116 ± 49 | $3.5 \pm 1.3 \times 10^{12}$ | 13 ± 4 |
| Ad5 | 3.8 | $3.6 \pm 0.5 \times 10^{11}$ | 117 ± 16 | $3.5 \pm 0.8 \times 10^{12}$ | 11 ± 2 |
| Ad5 | 3.4 | $4.2 \pm 0.8 \times 10^{11}$ | 83 ± 17 | $1.3 \pm 0.1 \times 10^{12}$ | 26 ± 3 |
| Ad3 | 1.4 | $8.1 \pm 1.3 \times 10^{9}$ | 1,956 ± 427 | $4.9 \pm 1.5 \times 10^{10}$ | 307 ± 86 |
| Ad3 | 1.7 | $8.3 \pm 1.8 \times 10^{9}$ | 2,147 ± 582 | $7.7 \pm 0.6 \times 10^{10}$ | 221 ± 16 |
| Ad7 | 1.9 | $2.3 \pm 0.5 \times 10^{9}$ | 8,217 ± 1,294 | $6.4 \pm 1.2 \times 10^{10}$ | 310 ± 63 |
| Ad7 | 1.6 | $4.1 \pm 0.5 \times 10^{9}$ | 3,969 ± 478 | $3.8 \pm 0.4 \times 10^{10}$ | 424 ± 41 |

[a] Cell monolayers were infected with serial dilutions of adenovirus inoculum of known virion concentration.
[b] The number of physical particles (PP) per ml of inoculum was determined by protein assay, assuming that the mass of one single adenovirion is $2.9 \times 10^{-16}$ g (24).
[c] Estimated by the fluorescent focus assay (17). R represents the ratio of physical to infectious particles in each inoculum, as assayed on both cell lines tested.

A549 cells were found to be fully permissive to human adenoviruses and to produce higher yields of virus progeny than did HeLa and KB cells in lytic cycle (unpublished observation). The higher infectivity efficiency observed for all serotypes in A549 cell monolayers (Table 1) and the clear and distinct pattern of A549 cell cytoskeletal network in immunofluorescence staining led us to preferentially use this cell line in the following biochemical experiments and to systematically use it in all of our cytological studies. The ratio of infectious to physical particles was thus a fundamental parameter of our analysis. In all of our experiments involving cell receptors and cell penetration of adenovirus particles, comparative analyses between adenovirus serotypes were performed by using the same number of physical virus particles per cell, regardless of the number of infectious virions present in the inoculum.

**(ii) Comparative study of receptor sites and binding constants for attachment of Ad2 and Ad3 at the surface of human cells.** The higher infectivity efficiency of both Ad3 (or Ad7) and Ad2 (or Ad5) on A549 than on KB cells reflected a higher degree of competency of the former cells for adenovirus infection. This phenomenon might occur at different levels and at different stages in the virus lytic cycle. It could possibly involve a higher efficiency in transcription or translation of early or late viral messages as well as even later events in the infectious cycle, such as protein processing, assembly, and maturation of the virions. However, the observed phenomenon could also be due to earlier virus-host cell interactions, i.e., adsorption on surface receptors or penetration through the cell membrane.

To address this question, the number of cell receptors for adenovirus on the cell surface and their affinity for adenovirions were determined from binding experiments, using graphical representation of the data (51). The average number of adenovirus receptor sites was found to range between 5,000 (Ad2) and 7,000 (Ad3) on KB and A549 cells (Fig. 1). Although the number of sites appeared to be slightly higher for Ad3 than for Ad2 with both cell lines analyzed (Fig. 1), there was no significant difference in the number of sites between KB and A549 for each serotype considered. The data obtained with Ad2 were therefore consistent with the results reported in previous studies, in which 3,000 to 6,000 receptor sites for Ad2 have been estimated to be present at the surface of HeLa cells (47, 48).

The apparent association constants per site ($K_{app}$) were estimated to be $9.2 \times 10^9$ $M^{-1}$ and $8.0 \times 10^9$ $M^{-1}$ for Ad2 with KB and A549 cells, respectively. A value of $9.1 \times 10^9$ $M^{-1}$ for $K_{app}$ was obtained for Ad3 with both cell types. Values ranging from $10 \times 10^9$ to $20 \times 10^9$ $M^{-1}$ for the intrinsic binding constant of Ad2 with HeLa cells have been previously reported (48). A discrete downward curvature of the Scatchard plots (Fig. 1) was reminiscent of the slightly positive cooperative binding already observed at temperatures above 20°C (48). In conclusion, the difference of 1 log in infectivity efficiency between adenoviruses of serotypes B and C could not be explained simply by a higher efficiency of adsorption at the cell surface. The association constants for the binding reactions of Ad2 and Ad3 with their receptor sites were found to be of the same order of magnitude for both serotypes with both cell lines. The number of receptor sites was also found to be similar for both cell types with each serotype considered. The difference thus resided in another step of the adenovirus cycle.

**(iii) Absence of interserotypic competition between adenoviruses of subgroups B and C for cell membrane receptors.** It is generally agreed that adenovirions can compete with each other within the same subgroup, e.g., Ad2 with Ad5 and Ad3 with Ad7, and also that homotypic or heterotypic inhibition of cellular adsorption of adenovirus particles can occur with soluble fiber capsomers of the same serotype or the same subgroup (reviewed in references 8 and 9). To determine whether the receptor sites were identical in nature for serotypes of subgroups B and C, we performed assays of homotypic and heterotypic inhibition of infection between two representative members of subgroups B and C, serotypes 2 and 3. Virions of mutant H2 *ts*1 or soluble Ad2 fibers were used as competitors for wild-type Ad2 (WT Ad2) or WTAd3 virions. H2 *ts*1 virions produced at 39°C are noninfectious (65) and therefore did not interfere with the value of the virus progeny yields in coinfection experiments. Furthermore, the coinfections were conducted at the nonpermissive temperature (39°C), and virus titers were corrected by subtracting the values obtained with single infections with H2 *ts*1 at 39°C, which represented the leak of the *ts*1 mutation. A strong homotypic inhibition occurred between H2 *ts*1 and WTAd2: virus production was reduced by a factor of about 300 at an H2 *ts*1-to-WTAd2 ratio of 50 and by a factor of almost 7,000 at a ratio of 100 (Table 2). No significant inhibition occurred between H2 *ts*1 and Ad3: a twofold decrease in Ad3 yields was obtained at a ratio of 1,000 with the competing H2 *ts*1.

The absence of competition for receptor sites between

TABLE 2. Homotypic and heterotypic competition between adenoviruses of subgroups C and B for A549 cell receptors[a]

| Infectious virus WTAd2 or WTAd3 (FFU/cell) | Competitor H2 *ts*1 (PP/cell) | Ratio, *ts*/WT (PP/FFU) | Titer (FFU/cell) | |
|---|---|---|---|---|
| | | | Homotypic, WTAd2 | Heterotypic, WTAd3 |
| 200 | 0 | | 22,000 | 1,711 |
| 100 | 0 | | 8,888 | 1,066 |
| 200 | 10,000 | 50 | 75 | 1,177 |
| 100 | 10,000 | 100 | 1.3 | 777 |
| 40 | 10,000 | 250 | 0 | 555 |
| 20 | 10,000 | 500 | 0 | 533 |
| 10 | 10,000 | 1,000 | 0 | 600 |

[a] Samples of A549 cell cultures ($4.5 \times 10^6$ cells) were incubated for 1 h at 25°C in the absence or presence of constant input (10,000 physical particles [PP] per cell) of noninfectious particles of mutant H2 *ts*1 produced at 39°C (nonpermissive temperature). Cells were then infected with WTAd2 (homotypic competition) or WTAd3 (heterotypic competition) at MOIs ranging from 10 to 200 FFU per cell. Cells were harvested and lysed 40 h after infection at 39°C, and virus titers of the cell lysates were determined. Standard error of the mean = 19 to 24% of the titer values.

virions of Ad2 and Ad3 was further confirmed by experiments using purified, soluble fiber of serotype 2 as a competitor. Considering that the molecular mass of Ad2 fiber in its native state is 165 to 180 kilodaltons (kDa) (7), the mass of one fiber is $2.7 \times 10^{-19}$ to $3.0 \times 10^{-19}$ g. The number of receptor sites for adenovirus-soluble fibers at the surface of HeLa cells has been estimated to be about $10^5$ per cell (47). To saturate the cell receptors, 10 μg of purified Ad2 fiber was added per $3 \times 10^6$ cells, corresponding to ca. 100 molecules of fiber per receptor site. When KB cell monolayers were incubated with Ad2 fiber for 2 h at 37°C before addition of adenovirus inoculum, no effect on Ad3 production was observed, whereas virus progeny decreased by a factor of 80 to 100 for Ad2 (data not shown). This latter result confirmed previous data on homotypic competition between Ad2 virions and its own fiber (49).

Our results therefore suggest that Ad2 fibers, either occurring as free capsid elements or present on Ad2 virus particles, recognize receptor components different from those binding to Ad3 virions. This conclusion implies that receptors are different for serotypes of subgroup B and serotypes of subgroup C.

**(iv) Absence of capping of rhodamine-labeled virions of serotype 3 (or 7) at the cell surface.** It has been shown that HeLa cells infected with rhodamine-labeled Ad2 present a pattern of fluorescent clusters often localized at one end of the cells (47). This immunofluorescence pattern suggested capping of virus-bound receptors at the cell surface, and it confirmed the rearrangement and aggregation of 7-nm intramembranous particles in the plane of the plasma membrane that we observed in freeze-fracture analysis of Ad2-attached cells (28, 29). Rhodamine-labeled Ad3 and Ad2 were adsorbed onto A549 cells under the conditions described in Materials and Methods, transferred to 37°C, fixed, and examined by immunofluorescence microscopy.

A clustering of fluorescent patches was visible at the surface of Ad2-infected cells, often asymmetrically localized at one pole of the cell (Fig. 2a). This fluorescence pattern was totally different from that of Ad3-infected cells, in which capping was never observed, even after 30 min of transfer to 37°C, and cells exhibited a random distribution of discrete granular patches at their surface (Fig. 2b). Mutant H2 *ts*1 behaved similarly to WTAd2 (not shown). The adenovirus-induced alterations of the infected cell plasma membrane

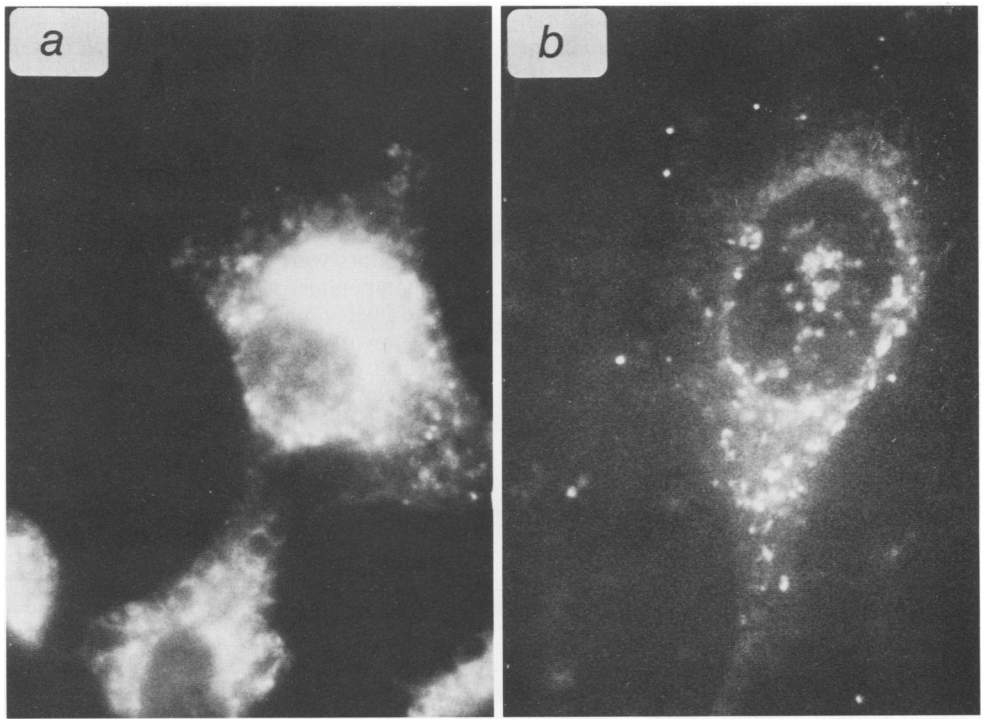


FIG. 2. Immunofluorescence analysis of attachment of adenovirus to A549 cells. Cell monolayers were incubated with adenovirus inoculum for 30 min at 4°C and with 5,000 rhodamine-labeled virions per cell. After removal of unadsorbed virus particles, cells were transferred to 37°C and further incubated at this temperature for 10 min. (a) Ad2; (b) Ad3.

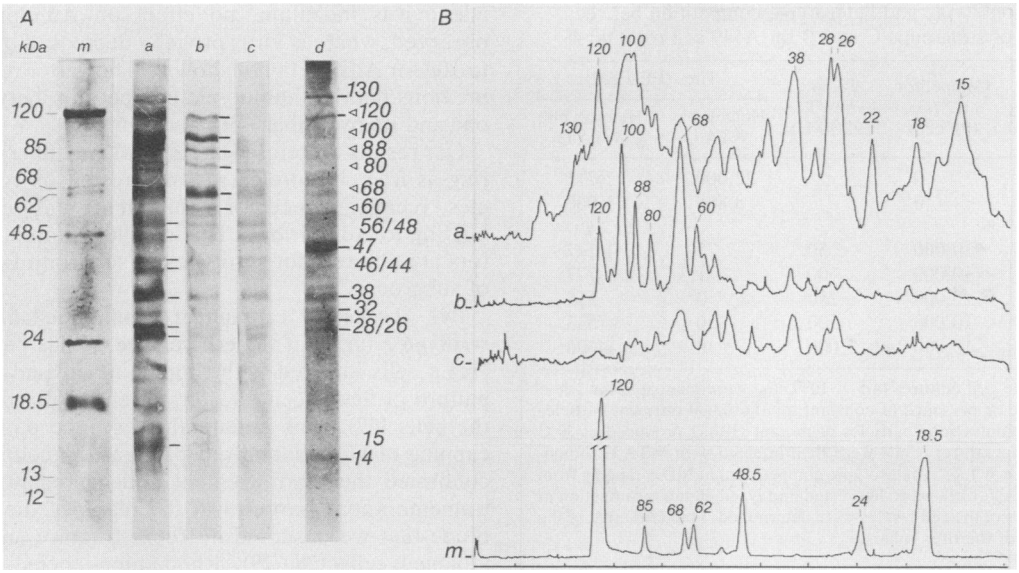


FIG. 3. Affinity labeling of KB cell plasma membrane receptors by adenovirions in a ligand overlay blotting technique. KB cells ($2 \times 10^9$ cells; 5 liters of a Spinner culture at $4 \times 10^5$ cells per ml) were processed for plasma membrane isolation. Assuming the presence of $10^4$ receptor sites per cell and a recovery of 50%, an equivalent of $10^{11}$ receptor sites was analyzed per lane in an SDS-containing 15.5% polyacrylamide gel. The membrane polypeptides were electrically transferred to nitrocellulose membrane, and the membrane was cut longitudinally into strips. Each strip was incubated with [$^{14}$C]valine-labeled adenovirions at high specific activity ($3 \times 10^7$ cpm/$10^{13}$ virions) in 1 ml of blotting buffer ($1.2 \times 10^5$ cpm per strip, corresponding to $4 \times 10^{10}$ particles) in the absence (lanes a and d) or presence (lanes b and c) of competing Ad2 fiber. Lane m, [$^{14}$C]valine-labeled adenovirus polypeptide markers transferred onto the same blots; lanes a to c, affinity labeling by Ad2; Lane d, affinity labeling with Ad3 virions. Lanes b and c, Competition between labeled Ad2 virions and unlabeled Ad2 fibers at $3.3 \times 10^{14}$ (b) or $1.6 \times 10^{15}$ (c) molecules of fibers per strip. Lines beside lane a indicate bands labeled by Ad2 that were efficiently competed for by unlabeled fiber at low concentration (i.e., 130, 56, 48, 46/44 doublet, 38, 28/26 doublet, and 15 kDa). Lines beside lane b represent major polypeptide bands efficiently labeled by Ad2 and quenched only by unlabeled fiber at high concentrations. Their apparent molecular masses are indicated by arrowheads at the right (120, 100, 88, 80, 68, and 60 kDa). Lines beside lane d represent major polypeptides labeled by Ad3. (A) Autoradiogram of the blots; (B) densitometric tracing of the corresponding lanes.

therefore appeared to be significantly different for Ad2 and Ad3. Taken together, the results of heterotypic competition of adsorption between Ad2 and Ad3 and the absence of capping of Ad3 at the cell surface strongly suggested that the receptor sites, as well as their routes of entry into host cells, were physiologically distinct for members of adenovirus subgroups B and C. The next set of experiments was designed to determine whether the receptor sites for Ad3 and Ad2 were also different at the polypeptide level.

**(v) Analysis of adenovirus receptor polypeptides by ligand overlay affinity blotting.** KB cell plasma membrane polypeptides were electrophoresed in SDS-polyacrylamide gels and electrically blotted onto nitrocellulose membranes. Blots were cut longitudinally, and blot strips were probed with [$^{14}$C]valine-labeled Ad3 or Ad2 virions. Figure 3A shows an autoradiogram of KB cell membrane polypeptides bound to labeled adenovirus particles in the ligand overlay technique. The patterns of affinity-labeled polypeptides were significantly different for Ad3 and Ad2.

The major bands in the Ad3 pattern were a 47-kDa protein species and a group of four discrete bands migrating between 38 and 26 kDa, clearly detectable over the background (Fig. 3A, lane d). In the Ad2 pattern, however (Fig. 3A, lane a), multiple bands with a similar intensity of labeling were visible in the range of 120 to 26 kDa in apparent relative molecular mass. Other significantly labeled polypeptide species were seen at 22, 18, and 15 kDa. Four protein bands with approximate molecular masses of 38, 32, 28, and 26 kDa seemed to be comigrating species in both Ad3 and Ad2 patterns (Fig. 3A, lanes a and d). In the higher-molecular-mass range, bands at 130 and 120 kDa, as well as minor discrete species in the ranges of 78 to 68 and 60 to 50 kDa, were also visible on both patterns. The possibility that some of the polypeptides of lower molecular mass represented proteolytic products from higher-molecular-mass species was unlikely for two reasons: (i) membrane samples were heated in SDS–2-mercaptoethanol–urea sample buffer immediately after isolation, and (ii) phenylmethylsulfonyl fluoride, tosyl-L-phenylalanyl chloromethyl ketone, and aprotinin were added throughout the fractionation procedure as protease inhibitors, and no difference was observed when one or all inhibitors were omitted.

A polypeptide pattern identical to the one exhibited with WTAd2 was obtained with mutant H2 *ts*1 produced at 39°C (not shown), suggesting that the recognition of membrane proteins by labeled adenovirions on blots was not dependent on the genetic competency of the virion. These results also suggested that the receptor sites for Ad3 and Ad2 significantly differed in polypeptide composition, although certain discrete polypeptide species were found to react with both serotypes. These latter polypeptides might represent common structural components of the viral receptor sites.

**(vi) Ligand overlay competition blotting.** Actin filaments are anchored to the plasma membrane and can be coextracted with membrane components. The apparent molecular mass of actin subunit is 42 to 46 kDa in SDS-polyacrylamide gels, very close to the value of 47 kDa found for the major Ad3-binding membrane protein. Considering the lack of accuracy of molecular mass determination in SDS-polyacrylamide gels, the 47-kDa species might represent actin polypeptide subunit. To test this hypothesis, the blots were saturated with antiactin antibody before ligand overlay blot-

ting with radioactive Ad3. There was no detectable quenching by antiactin antibody of the virus label bound to 47 kDa (not shown), suggesting that the Ad3 affinity-labeled membrane protein, present as a major 47-kDa band in the Ad3 pattern and as a minor species in the Ad2 pattern, was different from the actin subunit.

Ligand overlay competition blotting was also performed to assess the specificity of recognition between adenovirus particles and membrane proteins immobilized on blots. Unlabeled fiber and $^{14}C$-labeled virions labeled at a high specific activity were used in competition reactions with electrically transferred plasma membrane proteins. Two concentrations of serotype 2 fiber were incubated with the same blots, competing with the same amount of labeled Ad2 or Ad3 virions.

We found that Ad2 label was competed for by cold homotypic fiber. At a virion-to-fiber ratio of 1:8,000 (in terms of number of particles and molecules), the 130-kDa species and all bands migrating between 56 and 15 kDa were quenched (Fig. 3; compare lanes a and b in panel A and tracks a and b in densitometric tracings of panel B). Major bands still visible on blots were two strongly labeled species at 100 and 68 kDa and four other discrete bands at 120, 88, 80, and 60 kDa (Fig. 3A, lane b; Fig. 3B, track b). These six polypeptides were quenched only at higher concentrations of fiber (virion-to-fiber ratio of 1:40,000) (compare lanes b and c in Fig. 3A and tracks b and c in Fig. 3B). They might therefore represent adenovirus receptor components with a high affinity for Ad2 fiber and hence a high specificity for binding with virions of serotype 2. The bands still visible on the autoradiograms at high fiber concentrations (Fig. 3A, lane c; Fig 3B, track c) might correspond to membrane proteins bound to viral components other than fiber projections.

Competition experiments could not be performed between labeled and unlabeled Ad2 virions or at higher concentrations of Ad2 fibers because of the limited solubility of these ligands compared with the number of potential receptor sites analyzed on blots. Similarly, the low yield of soluble fibers in Ad3 infections made it impossible to perform homotypic competition between labeled Ad3 virions and unlabeled Ad3 fibers. However, no displacement of the Ad3 label from the major 47-kDa band was observed with competing serotype 2 fiber, even at high concentrations of Ad2 fiber (not shown).

**Adenovirus penetration and cointernalization of macromolecules with virions of different serotypes during the early stages of viral infection. (i) Penetration and compartmentalization of different adenovirus serotypes in A549 cells.** [$^3H$]thymidine-labeled adenovirus was incubated with A549 cells for 45 min at 37°C. Cells were washed, fixed with the reversible cross-linking reagent dithiobispropionimidate dihydrochloride (DTBP), and fractionated as previously described (3, 4). Radioactivity was assayed in the following compartments: (i) cytosol, containing soluble vimentin and other soluble cytoskeletal proteins; (ii) membranes and endocytotic vesicles; (iii) cytoskeletal network; and (iv) nucleus and residual insoluble matrix.

Ad3 seemed to adsorb to the A549 cell surface at a higher efficiency than did Ad2, with or without fixation by DTBP (Table 3). This result confirms our finding of a higher apparent number of receptor sites for Ad3 than for Ad2 (Fig. 1). However, for both serotypes, the number of virus particles adsorbed was lower than expected. If there are 5,000 Ad2 and 7,000 Ad3 receptors per cell, each of which takes 1 virion across the plasma membrane and 30,000 virions per cell were used, then approximately 17% of the Ad2 label and 23% of the Ad3 label should have been taken up. The number of cell-adsorbed virions never exceeded 10% of the input for Ad2 and 15% for Ad3 in different experiments, suggesting the existence of altered or incompetent virions within both serotype stocks.

TABLE 3. Recovery of [$^3H$]thymidine-labeled adenovirus particles in different cell compartments[a]

| Fraction | Ad2 | | Ad3 | |
|---|---|---|---|---|
| | cpm | % of adsorbed | cpm | % of adsorbed |
| Inoculum | 800,000 | | 800,000 | |
| Unfixed cells | 19,040 | | 95,894 | |
| DTBP-fixed cells | 15,740 | 100.0 | 52,133 | 100.0 |
| Cytosol | 8,106 | 51.5 | 3,371 | 6.4 |
| Endosomes and membranes | 3,052 | 19.4 | 15,014 | 30.5 |
| Cytoskeleton | 240 | 1.5 | 17,813 | 34.2 |
| Nuclear pellet | 4,348 | 27.6 | 15,035 | 28.8 |

[a] Adenovirus-infected A549 cells ($10^7$ cells; 20,000 to 30,000 particles per cell) were harvested at 45 min after infection at 37°C, fixed with DTBP, and fractionated as described in Materials and Methods. Cellular fractions were processed for acid-precipitable radioactivity, and radioactivity was counted in a liquid scintillation spectrometer.

For both serotypes, 28 to 30% of the bulk of adsorbed particles was recovered in the nuclear and insoluble fractions after 45 min at 37°C. However, major differences were found in the amount of virus particles recovered in the other fractions: about 50% of Ad2 was recovered in the cytosol, versus 6% for Ad3. In contrast, endosomes, reticulum, and insoluble network contained more than 60% of the infecting Ad3 particles and only 20% of the Ad2 particles. It seemed unlikely that the difference observed between the two serotypes might have resulted simply from some degradation of the labeled viral DNA used as a virus tracer within certain cell compartments, since the incubation time was only 45 time at 37°C and intact Ad7 DNA has been extracted from HeLa cell lysosomes as late as 2 h after infection at 37°C (44). Moreover, viral DNA was been found to be remarkably stable within H5 *dl*312-infected A549 cells (50). Rather, our biochemical data suggested that both members of subgroups B and C were transported to the nucleus with similar efficiency, although by different routes. This finding confirmed previous microscopic observations (13).

**(ii) Augmentation of cell permeability to impermeable macromolecules with adenoviruses of different serotypes.** Internalization of macromolecules was quantitatively analyzed by the HRP assay. Cells in monolayers or spinner cultures were infected with various adenovirus serotypes in the presence of HRP in the culture medium. RITC-HRP was used to control the cellular penetration of the enzyme on duplicate sets of infected cell cultures. For all cell lines studied, Ad2 and Ad3 increased their permeability to HRP by a factor of 1.7 to 2.3 (Table 4). A higher rate of spontaneous HRP internalization was observed in cells grown in suspension than in cells grown as monolayers, but adenovirus virions increased their permeability by a similar factor (1.5 to 1.7). Heat inactivation of virions for 30 min at 45°C abolished the adenovirus-induced augmentation of HRP internalization. Noninfectious H2 *ts*1 virions produced at 39°C induced the same increase in cellular HRP capture as did the WT serotypes 3 and 2. This result suggested that the augmentation of HRP internalization by the cell depends on the integrity of the capsid structure of the inoculated virions and not on their genetic competency and multiplication capacity.

TABLE 4. Augmentation of cell permeability to HRP induced by various adenovirus serotypes[a]

| Virus input | Peroxidase activity[b] | | | |
|---|---|---|---|---|
| | HeLa | HEp-2 | A549 | KB |
| Mock inoculum | 3.0 (1.0) | 7.2 (1.0) | 12.1 (1.0) | 153 (1.0) |
| WTAd5 | 6.7 (2.3) | 15.4 (2.1) | 21.1 (1.7) | 236 (1.5) |
| HI-Ad5[c] | 3.7 (1.2) | 7.2 (1.0) | 6.8 (0.7) | 158 (1.0) |
| WTAd3 | 6.3 (2.1) | 15.1 (2.1) | 27.1 (2.2) | 227 (1.5) |
| HI-Ad3[c] | ND | ND | 10.5 (1.0) | 170 (1.1) |
| H2 *ts*1 | ND | ND | 26.0 (2.1) | 256 (1.7) |

[a] Cell monolayers (HeLa, HEp2, and A549) and cells in suspension (KB) were infected at 5,000 physical particles per cell for 30 min at 37°C in the presence of RITC-HRP. The cells were extensively rinsed and processed for HRP assays.

[b] Expressed as $10^{-3}$ enzyme units per milligram of protein present in cell lysates. Figures in parentheses are ratios of activity in infected versus mock-infected cells. Standard error of the mean = 4 to 9% of the activity values. ND, Not determined.

[c] Heat-inactivated virions (45°C for 30 min), used at the same ratios of number of physical particles to cell as the WT.

**(iii) Difference in endosome lysis and cytoplasmic route between adenoviruses of different serotypes.** Qualitative analysis of cointernalization of macromolecules with adenovirus was performed by using immunofluorescence microscopy on A549 cells infected with Ad3 or Ad2 in the presence of RITC-HRP or FITC-dextran added to the virus inoculum. In control experiments, cell monolayers were infected with TRITC-labeled WTAd3 or WTAd2 and examined by fluorescence microscopy. RITC-HRP stayed within the endosomal vesicles after coentry with WTAd3 (Fig. 4b) or with H2 *ts*1 (not shown). In contrast, cells became totally fluorescent after 30 min of cointernalization of RITC-HRP with WTAd2 (Fig. 4a). This fluorescence pattern resulted from a lysis of the endosomal membranes, releasing RITC-HRP within the cytoplasm of infected cells. The same distinct patterns with WTAd3 and WTAd2 were observed when FITC-dextran was used in lieu of RITC-HRP (Fig. 4c and d).

Subgroup C adenoviruses have been shown to preferentially use the cytoplasmic route after cellular internalization (13, 42, 60–62), whereas subgroup B members are sequestered in large numbers within phagosomes (14). This finding was confirmed by our cell fractionation experiments with A549 cells infected with WTAd3 or WTAd2 (Table 3). From our experimental data (Table 4), we concluded that cellular permeability to macromolecules was quantitatively increased with all adenovirus serotypes studied except when virus capsids were heat denatured. This phenomenon resulted from the coentry of macromolecules and virus particles into endocytotic vesicles and was independent of the main route used by adenovirus to reach the nucleus. However, we observed a second phenomenon that was a massive release of macromolecules into the cytoplasm. This release occurred only with adenovirus serotypes whose infectious virions migrate through the cytoplasm after endosome lysis, i.e., WTAd2 or WTAd5, both members of subgroup C. Increased endocytosis of macromolecules and release of virions from the endosomes into the cytoplasm therefore seemed to be uncoupled events in adenovirus-infected cells.

**Cytoskeletal alterations during the early stages of adenovirus infection with various serotypes and modified virus particles. (i) Serotype dependence of vimentin proteolysis.** In two previous studies, we showed that vimentin was associated with intracytoplasmic migrating Ad2 particles (3) and that vimentin was proteolyzed by a $Ca^{2+}$-dependent, leupeptin-sensitive cellular protease activated early after adenovirus infection (4). Proteolysis of vimentin was found to be independent of the multiplicity of infection (MOI) for MOIs higher than $10^2$ FFU per cell. However, vimentin proteolysis was found to depend on the serotype of infecting adenovirus: Ad2, Ad5, Ad4, and Ad9 induced similar vimentin processing, whereas Ad3, Ad7, and Ad12 had no effect (4). Since subgroup C adenoviruses transit mainly through the cytoplasm and subgroup B adenoviruses are sequestered within the phagosomes of the infected cell, our next experiment was designed to test whether activation of the vimentin-specific protease was directly related to the cytoplasmic route of the infecting adenovirions. A549 cell monolayers were infected with various adenovirus serotypes, mutant particles, or physically altered WT virions at a constant input of 1,000 physical particles per cell. The virus inocula consisted of WTAd2, WTAd3, mutant H5 *dl*312, deleted in E1A (30), mutant H2 *ts*1, altered in the virus-coded protease (65), and heat-inactivated virions of WTAd2. Both H2 *ts*1 and heat-inactivated WTAd2 have been found to behave differently from their intact WT counterparts in infected cells: H2 *ts*1 virions produced at 39°C (43) and heat-inactivated WTAd2 virions (10) remain sequestered within the endocytotic vesicles as do serotypes of subgroup B (14, 44). No vimentin cleavage was evidenced in WTAd3-infected cells, whereas vimentin proteolytic products were visible in all other infected-cell samples analyzed in immunoblots with vimentin antiserum (data not shown). The fact that vimentin cleavage could occur with inactivated or uninfectious Ad2 virions that were blocked within the vacuoles strongly suggested that vimentin protease activation was serotype dependent and not viral route dependent.

**(ii) Viral route dependence of vimentin perinuclear condensation.** A549 cells were infected with various adenovirus serotypes at 1,000 virus particles per cell and examined by immunofluorescence microscopy, using antivimentin serum. Infection with WTAd3, H2 *ts*1, or heat-inactivated WTAd2 did not alter the pattern of the vimentin network (data not shown) as compared with the uninfected control cells (Fig. 5m). In contrast, in cells infected with infectious virions of WTAd2, other serotypes of subgroup C, or mutant H5 *dl*312, vimentin filaments had massively condensed around the nucleus. The condensation occurred progressively within the cells, detectable as early as 20 min after infection at 37°C, and was almost total after 45 min (Fig. 5f). These data suggested that the perinuclear condensation of vimentin occurring in adenovirus-infected cells was an early event depending on the presence of infectious adenovirions transiting through the cytoplasm.

Our biochemical and cytological analyses suggested that vimentin proteolysis occurring in adenovirus-infected cells depends on the adenovirus serotype. It is induced by serotypes belonging to subgroup C, e.g., WTAd2 and WTAd5, as well as by noninfectious particles of H2 *ts*1 or by heat-inactivated virions of WTAd2. In contrast, perinuclear condensation of the vimentin filament network in adenovirus-infected cells is not exclusively serotype dependent but viral migration dependent: noninfectious mutants of Ad2, heat-inactivated virions of Ad2 and Ad5, or serotypes of subgroup B (Ad3 and Ad7), which all remained sequestered in vesicles and reached the nucleus via the phagosomal route, failed to induce a detectable perinuclear condensation of vimentin (Table 5). Thus, the two events of vimentin cleavage on one

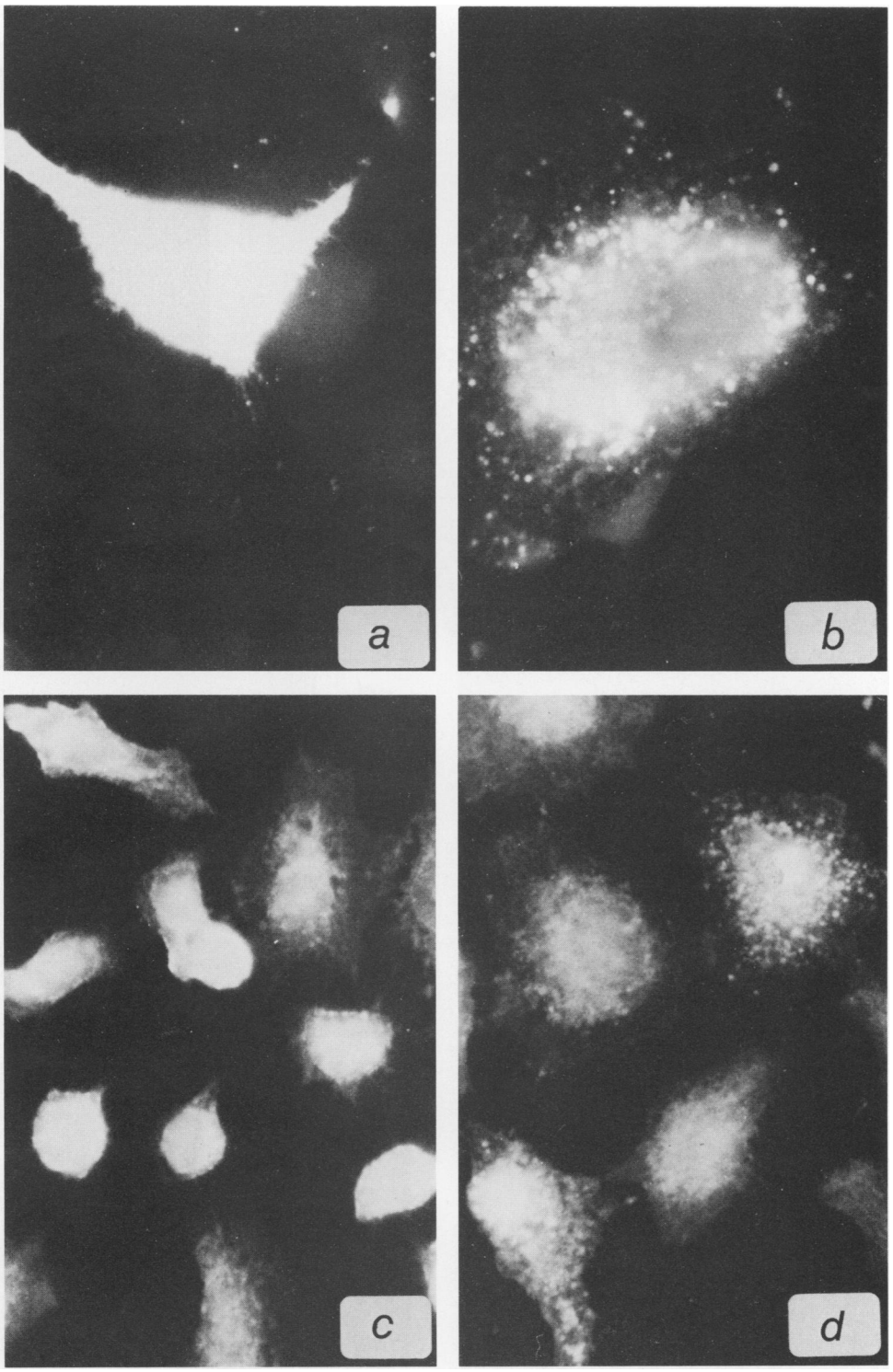


FIG. 4. Immunofluorescence analysis of cointernalization of macromolecules with adenovirus particles. A549 cell monolayers were incubated with RITC-HRP (a and b) or FITC-dextran (c and d) in the presence of WTAd2 (a and c) or WTAd3 (b and d) for 30 min at 37°C at 5,000 particles per cell. Cells were rinsed, fixed, and examined by immunofluorescence microscopy.

hand, and of vimentin condensation on the other hand, could be experimentally uncoupled in adenovirus-infected cells.

## DISCUSSION

We have used different adenovirus serotypes to analyze the mechanisms of adenovirus adsorption and penetration into host cells as well as the cytoskeletal alterations accompanying the entry and cellular migration of virions. We found significant differences between adenoviruses of subgroups B (Ad3 and Ad7) and C (Ad2 and Ad5). Quantitative and qualitative analyses of adenovirus binding with host cells showed that no competition occurred between Ad3 and Ad2

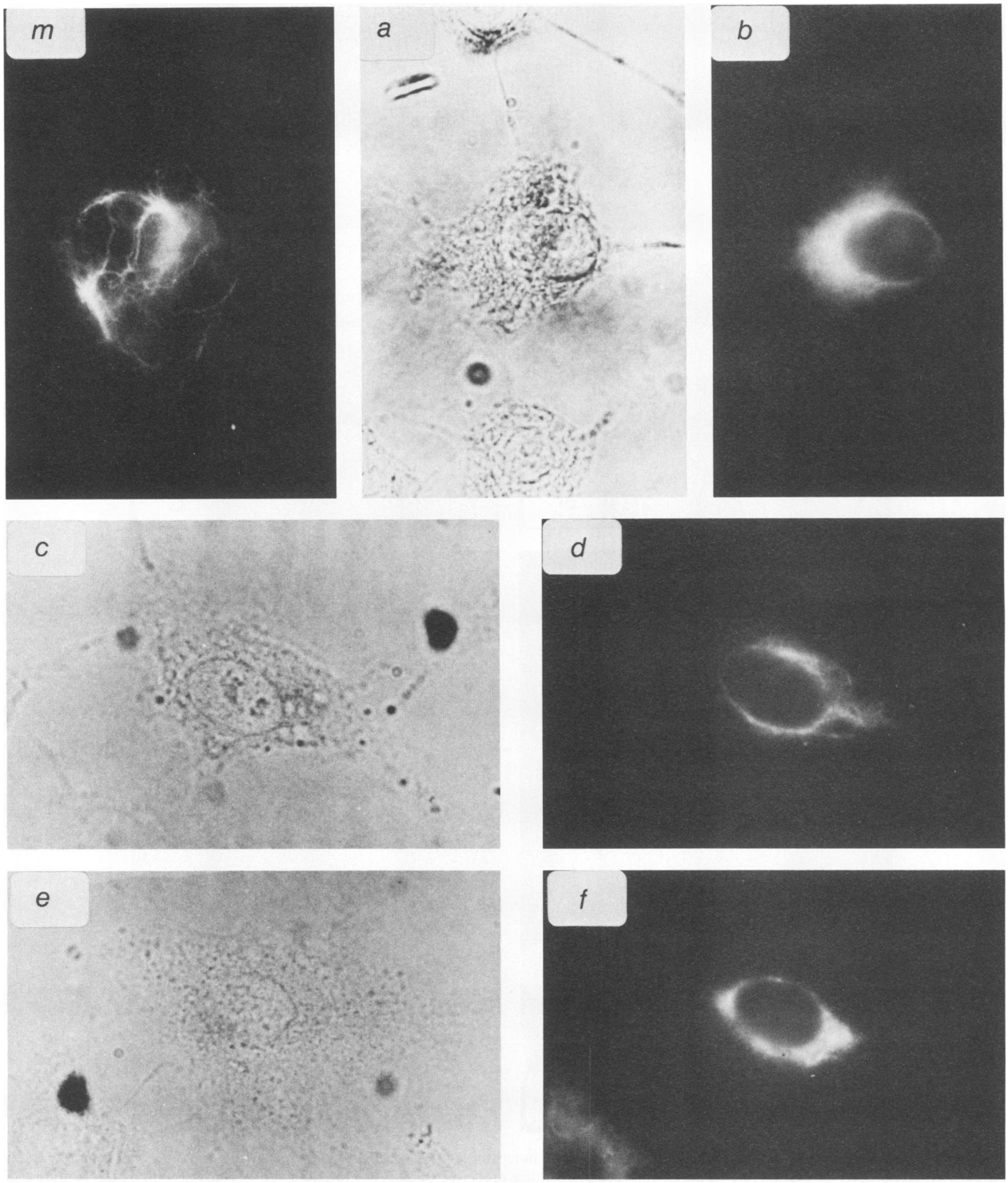


FIG. 5. Distribution of vimentin filaments in adenovirus-infected cells. A549 cell monolayers were infected with Ad2 at different times after infection at 37°C and at an equivalent ratio of virions to cell (2,000 virus particles per cell). Cell samples were processed and analyzed by double-label indirect immunofluorescence, using a mouse monoclonal antivimentin antibody. WTAd2-infected cells were examined at 15 (a and b), 30 (c and d), and 45 (e and f) min postinfection. a, c, and e, Phase-contrast microscopy; b, d, and f, immunofluorescence microscopy. Note the perinuclear condensation of the 10-nm vimentin filament network occurring in WTAd2-infected cells. The vimentin patterns of WTAd3-, H2 *ts*1-, and heat-inactivated Ad2-infected cells are not shown; they were all similar to the one observed in mock-infected cells (m).

TABLE 5. Influence of adenovirus serotypes and virus routes on host-cell alterations[a]

| Cellular process | Major localization of virions | | | | | | |
|---|---|---|---|---|---|---|---|
| | Cytoplasmic | | | Endosomal | | | |
| | WTAd2 | WTAd5 | H5 *dl*312 | WTAd3 | H2 *ts*1 | HI-Ad2 | HI-Ad5 |
| Endosome lysis | + | + | + | No | No | No | No |
| Vimentin condensation | + | + | + | No | No | No | No |
| Vimentin proteolysis | + | + | + | No | + | + | + |

[a] WTAd2, Wild-type virions of serotype 2; HI-, heat-inactivated virions (45°C for 30 min); H5 *dl*312, early mutant deleted in the E1A region of the Ad5 genome; H2 *ts*1, temperature-sensitive mutant of Ad2, mutated in the virus-coded protease and producing noninfectious, immature particles at 39°C.

virions (or Ad2 soluble fibers). Furthermore, capping at the cell surface was observed with Ad2 and Ad5 but was not detected with Ad3 and Ad7 (Fig. 2), suggesting that the adenovirus attachment and membrane modifications differed significantly between members of subgroups C and B.

KB cell membrane polypeptides were probed with $^{14}C$-labeled adenovirions in the ligand overlay blotting technique. Our results suggested that the major membrane polypeptides with an affinity for adenovirus particles in ligand blotting assays were different for Ad3 and Ad2. A major adenovirus-binding protein of 47 kDa was found on blots after incubation with Ad3, whereas multiple bands ranging from 130 to 15 kDa in apparent molecular mass were found to react with Ad2 (Fig. 3). Competition experiments between labeled Ad3 virions and unlabeled Ad2 fiber showed that the Ad3-reacting 47-kDa band was not displaced by Ad2 fiber.

The results of our competition assays between serotype 2 virions and homotypic fibers suggested the existence of at least two classes of cell membrane proteins with respect to Ad2 recognition and attachment. (i) The first consists of proteins with a low affinity for Ad2 fiber (or a low specificity of recognition), represented by bands migrating with apparent molecular masses ranging from 56 to 15 kDa. The label in these bands was drastically reduced at a competing fiber-to-virion ratio of 1:8,000 and might represent plasma membrane proteins binding nonspecifically to virions. (ii) In the second class are protein species with a high affinity (or specificity of binding) for Ad2 fiber, corresponding to the major bands visible on the autoradiograms at a fiber-to-virion ratio of 1:8,000 and almost totally chased at a ratio of 1:40,000. In the latter class, we identified two major bands at 100 and 68 kDa, respectively, and four less intense species at 120, 88, 80, and 60 kDa (Fig. 3A, lane b; Fig. 3B, track b). These proteins are candidates for serotype 2 fiber-binding components of human cell plasma membrane, thus confirming our previous investigation (27).

Svensson et al. have identified two glycoproteins of 40 and 42 kDa as the major components of the receptor site for Ad2 (62). This apparent discrepancy with our results might be explained by the fact that these authors had selected the membrane glycoproteins on a wheat germ lectin column before affinity chromatography on immobilized virions. In this case, they could have isolated one of the protein species identified on our autoradiograms as proteins with a rather low affinity for fiber and disappearing at low concentrations of competing fiber. Alternatively, they might have selected for membrane proteins reacting with virus capsid components other than fibers. Membrane preparations might still contain cytoskeletal elements underlying and attached to the plasma membrane. Also, we have found that hexon and core proteins can bind to cytoskeletal proteins immobilized on blots (3). Furthermore, the number of receptor sites has been estimated to be $10^5$ per cell for soluble fiber, versus $10^4$ for adenovirion (48). Fibers might thus attach to membrane components not accessible to virus particles or different from the ones recognized by virions.

On the basis of quantitative binding data, we calculated that receptor sites existed in quasiequivalent numbers for Ad3 and Ad2 at the surface of KB and A549 cells and that the apparent association constants with cellular receptors were also similar for Ad3 and Ad2 (Fig. 1). Since the architecture of the adenovirus receptor site is unknown, it is impossible to assess the role of each polypeptide in the recognition and binding of the virions. Our findings suggest that polypeptides different in nature might constitute a receptor site structurally or functionally adapted to adenovirions of different serotypes, with intrinsic binding constants of the same order of magnitude. If this is the case, it would explain why some heterologous recognition can occur between a given receptor site and two unrelated virus structures like human adenovirus fiber and coxsackievirus B3 (39), giving some molecular support to the theoretical concept of the receptor families (40).

We have previously shown that vimentin, a major component of the cytoskeletal intermediate filaments, is proteolytically processed at early stages of infection with Ad2 and Ad5 but not with Ad3, Ad7, and Ad12. This processing was likely due to the activation of a cellular, $Ca^{2+}$-dependent protease (4). We therefore analyzed the state of vimentin as a cytological and biochemical marker of adenovirus infection. Immunofluorescent staining showed that the vimentin filament network condensed around the nucleus of cells infected with Ad2 and Ad5. Vimentin processing and condensation thus occurred simultaneously in cells infected with Ad2 or Ad5, two serotypes that were mainly found transiting through the cytoplasm (14, 42, 60, 61). Neither of the two phenomena was observed with Ad3 or Ad7, two serotypes that were thought to utilize a phagosomic route to reach the nucleus (14, 44).

We originally concluded that vimentin cleavage and its perinuclear condensation were coupled events in adenovirus-infected cells and reflected the transcytoplasmic migration of infectious adenovirus particles. However, using various adenovirus serotypes, certain mutants, and inactivated forms of adenovirions, we found that vimentin proteolysis and vimentin perinuclear condensation could be experimentally uncoupled in adenovirus-infected cells. Proteolytic processing of vimentin was observed only during infection with members of subgroup C adenovirus (e.g., Ad2 or Ad5), regardless of (i) the integrity of the particles (intact or heat-inactivated WT virions and mutant H2 *ts*1 produced at 39°C), (ii) the genetic competency of the virions (mutants H2 *ts*1 and H5 *dl*312), and (iii) the cellular compartmentalization of the virions (endosomal H2 *ts*1 and heat-inactivated WTAd2, as well as cytoplasmic WTAd2). Thus, our observations had four implications at the cellular level: (i) vimentin proteolysis might occur in adenovirus-infected cells without necessarily being followed by a perinuclear condensation of the vimentin network; (ii) vimentin condensation was a cytological marker of cytoplasmic transit of adenovirus particles; (iii) vimentin processing appeared as an adenovirus serotype-dependent phenomenon and as a cellular marker of infection with subgroup C adenoviruses; and (iv)

inhibition of vimentin proteolysis by leupeptin reduced the adenovirus progeny yields for all serotypes showing a cytoplasmic transit (4), including fastidious serotypes 40 and 41 (data not shown). Since Ad40 and Ad41 are known to be highly pathogenic in children (31, 53, 64), this finding might represent a clue for a new class of antiviral drugs.

Cointernalization of impermeable macromolecules and adenovirus particles was also studied with various serotypes belonging to subgroups B and C. Using FITC-dextran and RITC-HRP, we confirmed that adenovirus infection provoked a higher permeability of host cells to macromolecules (19, 45, 54–56, 70). However, we discovered that the phenomenon of permeabilization was equally induced by Ad2 (or Ad5) and Ad3 (or Ad7), although their modes of cellular binding and entry were apparently different. Our biochemical and cytological data suggested that the increased cellular permeability induced by adenovirus in fact represented the global result of two distinct events: (i) cointernalization of macromolecules and virus particles and (ii) massive release of internalized macromolecules from the endosomes into the cytoplasm of the infected cells.

The first phenomenon was observed with all adenovirus serotypes studied and with noninfectious virions of mutant H2 *ts*1. It thus occurred as a serotype-independent process but required the integrity of the viral capsid: heat-inactivated virus particles failed to increase cell permeability (Table 4). It must be added that heat-inactivated particles of Ad2 or Ad5 competed with intact Ad2 or Ad5 virions (data not shown), suggesting similar modes of attachment. Penton base, which represents the most fragile structure of the capsid and the viral component involved in endosomal release of internalized drugs (55, 56), might be responsible for this requirement.

On the contrary, intracytoplasmic release of virions with cointernalized macromolecules was never observed with WTAd3, WTAd7, heat-inactivated WTAd2 (or WTAd5) virions, and H2 *ts*1 (Fig. 4). It was observed only with intact WTAd2 and WTAd5, whose infectious virions normally transit through the cytoplasm after lysis of the endosomal membranes (54, 56). This phenomenon therefore appeared to depend on three parameters: (i) adenovirus serotype, (ii) integrity of the viral capsid, and (iii) infectivity of the virions.

We are presently analyzing the fate of macromolecules cointernalized with Ad3 virions. If they can efficiently reach the nucleus along with the virus particles, then members of adenovirus subgroup B might serve to internalize drugs into endosomal vesicles and to pilot them toward possible specific nuclear targets. This internalization and cellular route would thus present two major advantages: (i) possible modification and activation by lysosomal enzymes of inactive drug precursor and (ii) minimizing the toxic effect toward cytoplasmic structures and functions.

## ACKNOWLEDGMENTS

We are grateful to Didier Petite for providing cell lines and cultures, to Jolanta Niewiarowska for valuable advice in immunofluorescent stainings, and to Bernard Gay-Heuzet for illustrations.

Work in Lille (by C.D., M.T.B., and M.L.C.B.) was supported by the Institut National de la Santé et de la Recherche Médicale (U-233) and the Fondation pour la Recherche Médicale. Work in Montpellier (by P.B.) was supported by grants from the Ligue du Cancer, the Association pour la Recherche sur le Cancer, the Conseil Régional du Languedoc-Roussillon, and the Agence Nationale de Recherche sur le SIDA.

## LITERATURE CITED

1. **Akusjärvi, G., and H. Persson.** 1981. Gene and mRNA precursor for polypeptide VI from adenovirus type 2. J. Virol. **38**:469–482.
2. **Allard, A. K., G. Wadell, K. M. Evander, and G. K. K. Lindman.** 1985. Specific properties of two enteric adenovirus 41 clones mapped within early region 1A. J. Virol. **54**:145–150.
3. **Belin, M. T., and P. A. Boulanger.** 1985. Cytoskeletal proteins associated with intracytoplasmic human adenovirus at an early stage of infection. Exp. Cell Res. **160**:356–370.
4. **Belin, M. T., and P. A. Boulanger.** 1987. Processing of vimentin occurs during the early stages of adenovirus infection. J. Virol. **61**:2559–2566.
5. **Berk, A. J.** 1986. Adenovirus promoters and E1A transactivation. Annu. Rev. Genet. **20**:45–79.
6. **Bhatti, A. R., and J. Weber.** 1979. Protease of adenovirus type 2: partial characterization. Virology **96**:478–485.
7. **Boulanger, P. A., and C. Devaux.** 1983. Native molecular weight of adenovirus proteins: on the oligomeric structure of the fiber. Biochem. Biophys. Res. Commun. **110**:913–918.
8. **Boulanger, P. A., and K. Lonberg-Holm.** 1981. Components of non-enveloped viruses which recognize receptors, p. 21–46. *In* K. Lonberg-Holm and L. Philipson (ed.), Receptors and recognition, series B, vol. 8. Virus receptors, part 2. Animal viruses. Chapman & Hall, New York.
9. **Boulanger, P. A., and L. Philipson.** 1981. Membrane components interacting with non-enveloped viruses, p. 117–139. *In* K. Lonberg-Holm and L. Philipson (ed.), Receptors and recognition, series B, vol. 8. Virus receptors, part 2. Animal viruses. Chapman & Hall, New York.
10. **Brown, D. T., and B. T. Burlingham.** 1973. Penetration of host cell membranes by adenovirus 2. J. Virol. **12**:386–396.
11. **Carrasco, L.** 1981. Modification of membrane permeability induced by animal viruses early in infection. Virology **113**: 623–629.
12. **Carrasco, L., and M. Esteban.** 1982. Modification of membrane permeability in vaccinia virus-infected cells. Virology **117**:62–69.
13. **Chardonnet, Y., and S. Dales.** 1970. Early events in the interaction of adenoviruses with HeLa cells. I. Penetration of type 5 and intracellular release of the DNA genome. Virology **40**: 462–477.
14. **Chardonnet, Y., and S. Dales.** 1970. Early events in the interaction of adenoviruses with HeLa cells. II. Comparative observations on the penetration of types 1, 5, 7, and 12. Virology **40**:478–481.
15. **Chatterjee, P. K., and S. J. Flint.** 1987. Adenovirus type 2 endopeptidase: an unusual phosphoprotein matured by autocatalysis. Proc. Natl. Acad. Sci. USA **84**:714–718.
16. **Dales, S.** 1962. An electron microscope study of the early association between two mammalian viruses and their hosts. J. Cell Biol. **13**:303–322.
17. **D'Halluin, J. C., M. Milleville, P. A. Boulanger, and G. R. Martin.** 1978. Temperature-sensitive mutant of adenovirus type 2 blocked in virion assembly: accumulation of light intermediate particles. J. Virol. **26**:344–356.
18. **Fernandez-Puentes, C., and L. Carrasco.** 1980. Viral infection permeabilizes mammalian cells to protein toxins. Cell **20**:769–775.
19. **FitzGerald, D. J. P., R. Padmanabhan, I. Pastan, and M. C. Willingham.** 1983. Adenovirus induced release of epidermal growth factor and *Pseudomonas* toxin into the cytosol of KB cells during receptor-mediated endocytosis. Cell **39**:607–617.
20. **Geidushek, P., and G. P. Tocchini-Valentini.** 1988. Transcription by RNA polymerase III. Annu. Rev. Biochem. **57**:873–914.
21. **Gershoni, J. M., and G. E. Palade.** 1983. Protein blotting: principles and applications. Anal. Biochem. **131**:1–15.
22. **Giard, D. J., S. A. Aaronson, G. J. Todaro, P. Arnstein, J. H. Kersey, H. Dosik, and W. P. Parks.** 1973. In vitro cultivation of human tumors: establishment of cell lines derived from a series of solid tumors. J. Natl. Cancer Inst. **51**:1417–1423.
23. **Green, M., M. Piña, and R. C. Kimes.** 1967. Biochemical studies on adenovirus multiplication. XII. Plaquing efficiencies of purified human adenoviruses. Virology **31**:562–565.

24. **Green, M., M. Piña, R. C. Kimes, P. C. Wensink, L. A. MacHattie, and C. A. Thomas, Jr.** 1967. Adenovirus DNA. I. Molecular weight and conformation. Proc. Natl. Acad. Sci. USA **57**:1302–1309.
25. **Helenius, A., M. Klielian, J. White, and J. Kartenbeck.** 1986. Prospects for antiviral agents which modify the pathway by enveloped viruses, p. 205–210. *In* R. L. Crowell and K. Lonberg-Holm (ed.), Virus attachment and entry into cells. American Society for Microbiology, Washington, D.C.
26. **Helenius, A., M. Marsh, and D. J. White.** 1980. The entry of viruses into animal cells. Trends Biochem. Sci. **5**:104–196.
27. **Hennache, B., and P. A. Boulanger.** 1977. Biochemical study of KB cell receptor for adenovirus. Biochem. J. **166**:237–247.
28. **Hennache, B., G. Torpier, and P. A. Boulanger.** 1979. Freeze-fracture study of adenovirus-induced KB cell surface alterations. Exp. Cell Res. **124**:139–150.
29. **Hennache, B., G. Torpier, and P. A. Boulanger.** 1982. Adenovirus adsorption and sterol redistribution in KB cell plasma membrane. Exp. Cell Res. **137**:459–463.
30. **Jones, N., and T. Shenk.** 1979. An adenovirus type 5 early gene function regulates expression of other early viral genes. Proc. Natl. Acad. Sci. USA **76**:3365–3369.
31. **Kidd, A. H.** 1984. Genome variants of adenovirus 41 (subgroup G) from children with diarrhaea in South Africa. J. Med. Virol. **14**:49–59.
32. **Kohn, A.** 1979. Early interactions of viruses with cellular membranes. Adv. Virus Res. **24**:223–276.
33. **Kruijer, W., F. M. A. van Schaik, and J. S. Sussenbach.** 1980. Nucleotide sequence analysis of a region of adenovirus 5 DNA encoding a hitherto unidentified gene. Nucleic Acids Res. **8**:6033–6042.
34. **Laemmli, U. K.** 1970. Cleavage of structural proteins during the assembly of the head of bacteriophage T4. Nature (London) **227**:680–685.
35. **Langanger, G., J. De Mey, M. Moeemans, G. Daneels, M. De Brabander, and J. V. Small.** 1984. Ultrastructural localization of α-actinin and filamin in cultured cells with immunogold staining (IGS) method. J. Cell Biol. **99**:1324–1334.
36. **Lenstra, J. A., and H. Bloemendal.** 1983. The major proteins from HeLa cells. Identification and intracellular localization. Eur. J. Biochem. **130**:419–426.
37. **Li, Q. G., and G. Wadell.** 1988. Comparison of 17 genome types of adenovirus type 3 identified among strains recovered from six continents. J. Clin. Microbiol. **26**:1009–1015.
38. **Liang, Y. K., G. Akusjärvi, P. Aleström, U. Pettersson, M. Tremblay, and J. Weber.** 1983. Genetic identification of an endoproteinase encoded by the adenovirus genome. J. Mol. Biol. **57**:217–222.
39. **Lonberg-Holm, K., R. L. Crowell, and L. Philipson.** 1976. Unrelated animal viruses share receptors. Nature (London) **259**:679–681.
40. **Lonberg-Holm, K., and L. Philipson.** 1974. Early interaction between animal viruses and cells. Monogr. Virol. **9**:1–148.
41. **Madshus, I. M., S. Olnes, and K. Sandvig.** 1984. Mechanism of entry into the cytosol of poliovirus type 1: requirement for low pH. J. Cell Biol. **98**:1194–1200.
42. **Miles, B. D., R. B. Luftig, J. A. Weatherbee, R. R. Weihing, and J. Weber.** 1980. Quantitation of the interaction between adenovirus types 2 and 5 and microtubules inside infected cells. Virology **105**:265–269.
43. **Mirza, M. A., and J. Weber.** 1979. Uncoating of adenovirus type 2. J. Virol. **30**:462–471.
44. **Ogier, G., Y. Chardonnet, and W. Doerfler.** 1976. The fate of type 7 adenovirions in lysosomes of HeLa cells. Virology **77**:67–77.
45. **Otero, N. J., and L. Carrasco.** 1987. Proteins are co-internalized with virion particles during early infection. Virology **160**:75–80.
46. **Otto, J. J.** 1985. Detection of vinculin-binding proteins with an $^{125}$I-vinculin gel overlay technique. J. Cell Biol. **97**:1283–1287.
47. **Persson, R., U. Svensson, and E. Everitt.** 1983. Virus receptor interaction in the adenovirus system. II. Capping and cooperative binding of virions on HeLa cells. J. Virol. **46**:956–963.
48. **Persson, R., C. Wohlfart, U. Svensson, and E. Everitt.** 1985. Virus-receptor interaction in the adenovirus system: characterization of the positive cooperative binding of virions on HeLa cells. J. Virol. **54**:92–97.
49. **Philipson, L., K. Lonberg-Holm, and U. Pettersson.** 1968. Virus-receptor interaction in an adenovirus system. J. Virol. **2**: 1064–1075.
50. **Ross, P. M.** 1989. Cellular and adenovirus *dl* 312 DNA metabolism in cycling or mitotic human cultures exposed to supralethal gamma radiation. J. Cell Biol. **109**:1993–2002.
51. **Scatchard, G.** 1949. The attraction of proteins for small molecules and ions. Ann. N.Y. Acad. Sci. **51**:660–672.
52. **Schlesinger, R. W.** 1969. Adenoviruses. The nature of the virion and of controlling factors in productive or abortive infection and tumorigenesis. Adv. Virus Res. **14**:1–61.
53. **Schmitz, M., R. Wigand, and W. Heinrich.** 1983. Worldwide epidemiology of human adenovirus infections. Am. J. Epidemiol. **117**:455–466.
54. **Seth, P., D. FitzGerald, H. Ginsberg, M. C. Willingham, and I. Pastan.** 1984. Evidence that the penton base of adenovirus is involved in potentiation of toxicity of *Pseudomonas* exotoxin conjugated to epidermal growth factor. Mol. Cell. Biol. **4**: 1528–1533.
55. **Seth, P., D. FitzGerald, M. C. Willingham, and I. Pastan.** 1986. Pathway of adenovirus entry into cells, p. 191–195. *In* R. L. Crowell and K. Lonberg-Holm (ed.), Virus attachment and entry into cells. American Society for Microbiology, Washington, D.C.
56. **Seth, P., I. Pastan, and M. C. Willingham.** 1985. Adenovirus-dependent increase in cell membrane permeability. J. Biol. Chem. **260**:9598–9602.
57. **Silver, L., and C. W. Anderson.** 1988. Interaction of human adenovirus serotype 2 with human lymphoid cells. Virology **165**:377–387.
58. **Stillman, B.** 1986. Functions of the adenovirus E1B tumor antigens. Cancer Surv. **5**:389–404.
59. **Stone, D. K., X. S. Xie, and E. Racker.** 1983. An ATP-driven proton pump in clathrin-coated vesicles. J. Biol. Chem. **258**: 4059–4062.
60. **Svensson, U.** 1985. Role of vesicles during Ad2 internalization into HeLa cells. J. Virol. **55**:442–449.
61. **Svensson, U., and R. Persson.** 1984. Entry of adenovirus 2 into HeLa cells. J. Virol. **51**:687–694.
62. **Svensson, U., R. Persson, and E. Everitt.** 1981. Virus-receptor interaction in the adenovirus system. I. Identification of virion attachment proteins of the HeLa cell plasma membrane. J. Virol. **38**:70–81.
63. **Takiff, H. E., S. E. Strauss, and C. F. Garon.** 1981. Propagation and in vitro studies of previously non-cultivable enteral adenoviruses in 293 cells. Lancet **ii**:832–834.
64. **Uhnoo, I., G. Wadell, L. Svensson, and M. E. Johansson.** 1984. Importance of enteric adenoviruses 40 and 41 in acute gastroenteritis in infants and young children. J. Clin. Microbiol. **20**:365–372.
65. **Weber, J.** 1976. Genetic analysis of adenovirus type 2. III. Temperature sensitivity of processing of viral proteins. J. Virol. **17**:462–471.
66. **Whitaker, J. R., and P. E. Granum.** 1980. An absolute method for protein determination based on difference in adsorbance at 235 and 280 nm. Anal. Biochem. **109**:156–159.
67. **Whyte, P., H. E. Ruley, and E. Harlow.** 1988. Two regions of the adenovirus early region 1A proteins are required for transformation. J. Virol. **62**:257–265.
68. **Wigand, R.** 1987. Pitfalls in the identification of adenoviruses. J. Virol. Methods **16**:161–169.
69. **Yamashiro, D. J., S. R. Fluss, and F. R. Maxfield.** 1983. Acidification of endocytic vesicles by an ATP-dependent proton pump. J. Cell Biol. **97**:929–934.
70. **Yoshimura, A.** 1985. Adenovirus-induced leakage of co-endocytosed macromolecules into the cytosol. Cell Struct. Funct. **10**:391–404.